Case Studies in Thermal Engineering 27 (2021) 101232

Contents lists available at ScienceDirect

Case Studies in Thermal Engineering

journal homepage: www.elsevier.com/locate/csite

Thermal, efficiency and power output evaluation of pyramid, hexagonal and conical forms as solar panel

Hamdi Ayed [a,b], Hazim Moria [c], Fayez Aldawi [c], Naeim Farouk [d,e], Kamal Sharma [f], Mohammad Mehdizadeh Youshanlouei [g,*], Ibrahim Mahariq [h], Fahd Jarad [i,j,**]

[a] Department of Civil Engineering, College of Engineering, King Khalid University, Abha, 61421, Saudi Arabia
[b] Higher Institute of Transport and Logistics of Sousse, University Sousse, Tunisia
[c] Department of Mechanical Engineering Technology, Yanbu Industrial College, Yanbu Al-Sinaiyah City, 41912, Saudi Arabia
[d] Mechanical Engineering Department, College of Engineering, Prince Sattam Bin Abdulaziz University, Alkharj, 16273, Saudi Arabia
[e] Mechanical Engineering Department, Faculty of Engineering, Red Sea University Port Sudan, Sudan
[f] Institute of Engineering and Technology, GLA UNIVERSITY, Mathura, U.P, 281406, India
[g] Sustainable Management of Natural Resources and Environment Research Group, Faculty of Environment and Labour Safety, Ton Duc Thang University, Ho Chi Minh City, Viet Nam
[h] College of Engineering and Technology, American University of the Middle East, Kuwait
[i] Department of Mathematics, Cankaya University, Etimesgut, Ankara, Turkey
[j] Department of Medical Research, China Medical University Hospital, China Medical University, Taichung, Taiwan

ARTICLE INFO

Keywords:
Solar panels
Power output
Cooling performance
Temperature distribution
Electric efficiency

ABSTRACT

Through the present investigation, the thermal and power output of novel-shaped solar panels are evaluated. For the cooling of the mentioned forms, forced air flow was utilized. Three novel shapes, of Pyramid, Hexagonal, and Conical which had the equal lateral surface were considered. For the simulation, an open source CFD software was utilized. The lateral surfaces were put under identical amount of heat flux. Air as the coolant fluid was injected with constant inlet temperature from the trapdoors at the bottom of different shaped structures. Three different values of heat flux and air injection rate were evaluated for each shape. The outcomes presented that the conical shaped solar panel exhibits better thermal performance than other geometries. Furthermore, conical form finds the least temperature that was about 10.5 °C less than that of the pyramid-shaped panel. Furthermore, it was revealed that the corners of pyramid and hexagonal-shaped solar panels have higher temperature. Also, it was found that the efficiency of conical shaped panel was up to 8.4% more than that of pyramid-shaped panel.

1. Introduction

Through the last decades, the rapid increment of the human population and the lack in energy sources has increased the importance on the investigations of the energy subjects. These investigations include different subjects as like to energy storing instruments [1,2], optimizing power production systems [3] and renewable energy sources [4,5]. Amongst various type of renewable energy sources, the use of solar energy has gained lots of attentions [6,7]. The Photovoltaic panels (PV) are the instruments that directly change the solar

* Corresponding author.
** Corresponding author. Department of Mathematics, Cankaya University, Etimesgut, Ankara, Turkey.
E-mail addresses: m.mehdizadeh.y@gmail.com (M.M. Youshanlouei), fahd@cankaya.edu.tr (F. Jarad).

https://doi.org/10.1016/j.csite.2021.101232
Received 24 March 2021; Received in revised form 10 June 2021; Accepted 6 July 2021
Available online 7 July 2021

energy to electrical energy and has gained the attentions of researchers and engineers in energy systems [8]. Recently, various designs of Photovoltaic (PV) solar panels have been introduced by experts [9]. The aim of these designs was to enhance the photovoltaic panels' efficiency. Different parameters affect the efficiency of PVs. However, the temperature of the back-side of the photovoltaic panel is critical parameter [10]. The reduction of back side temperature of PV panel significantly affects the efficiency of PVs. Increment in the back-side temperature by 1 °C can lead to a loss in efficiency of PVs by 0.5% [11]. Consequently, experts have attempted to use various methods and techniques to reduce the photovoltaics temperature. Cooling methods, such as water spraying, application of heat sink, forced water circulation, application of phase change materials, thermoelectric cooling systems, and forced air flow circulation, are commonly used for cooling PV models [12,13]. In the next paragraph, a brief summary of investigations that have been conducted on the cooling of solar models is presented.

One of the high-tech mechanisms for reducing the temperature of PV module involves the use of radiative cooling (RC). This method is based on a feature of certain substances that reflect the infrared waves. Specifically, the infrared waves play significant role in heating the PV modules [14]. When comparing with bare silicon cells, RCs can reduce the temperature of the cell up to 10 °*C* [15]. Lee and Luo [16] conducted an experiment and concluded that the usage of pyramid shaped structure of polydimethylsiloxane as thermal emitter may reduce the micro-crystalline-Si solar cells temperature by up to 16 °*C*. Long et al. [17] reported a reduction in the temperature of solar cells by 20 °C via a micro-grating RC surface, which consists of a thin layer of SiO_2.

Another cooling method is the convective cooling. This method can be categorized into hydro-based cooling and aero-based cooling as per the fluid that is used for cooling [18]. Experts have tried to use this method by integrating it with extended surfaces [19], nano-particles [20], and natural convection [21]. Salem et al. [22] experimentally studied the quality and quantity of affecting the hydro mechanism cooling on the performance of photovoltaics. The results indicated that hydro cooled photovoltaics exhibit higher electrical efficiency in comparison with pure photovoltaics. Abdallah et al. [23] employed the Al_2O_3/water nano-fluid for photovoltaic cooling and observed a great enhancement in the solar cells' efficiency based on the aforementioned mechanism. Subsequently, Abdallah et al. [24] added Multi Walled Carbon Nano Tubes (MWCNTs) to water and used this combination as a working fluid for cooling PV modules. The results indicated that combination of MWCNTs with water can improve the efficiency of the PV module by 29.23% when compared to that of obtained by using pure water. In later investigations, Alous et al. [25] compared the influence of adding MWCNTs and graphene nano-platelets to water for improving the efficiency of a PV module. Their results indicated MWCNTs can increase the photovoltaic modules efficiency when compared to that obtained from using graphene nanoplatelets. Sajjad et al. [26] proposed the exhaust air of an air conditioning system to be used as the coolant of the photovoltaic module. Their results indicated the aforementioned mechanism leads to improvement in the production of electrical power and performance ratio by 7.2% and 6%, respectively. Kabeel et al. [27] performed an experimental study and compared three mechanisms of cooling involving Hydro, Aero and Aero-Hydro cooling methods. Elminshawy et al. [28] examined the effect of a buried heat exchanger based on aero cooling technique on the performance of photovoltaic module. Through their study, they injected air with four flow rates of 0.0228, 0.0248, 0.0268, and 0.0288 m^3/s for cooling a PV module. Their results indicated a reduction in the photovoltaic module temperature by 29 °C when compared to that of non-cooling PV module. Wu et al. [29] reported that the position of cooling channel is very important in the thermal performance of the PVT panels. Through their investigations the cooling channel was fabricated on the top and bottom side of the PV panel. Xu et al. [30]investigated the performance of a PV panel integrated with two air cooling channel for a full day condition. Their results presented that in case of using two cooling channels, the thermal and electrical efficiency of the PVT panels would increase up to 57.3% and 10.2%, respectively. Through another investigation, Golzari et al. [31] evaluated the performance of PVT system which was cooled by corona wind. They reported that by using corona wind the total performance of the system would increase up to 28.9%. Amanlou et al. [32] reported that by using the uniform distribution of the cooling air flow, the electrical efficiency of the PVT panel could increase up to 36%. They reported that in case of none-uniform flow distribution, the local increments of the back side temperature significantly reduce the performance of the PVT panel.

The application of forced air flow circulation, due to the ease of fabrication of the cooling instruments and the availability and abundance of air, can be easily used by experts and engineers. In this method, the design parameters strongly influence the cooling performance of the aforementioned mechanism. In the present work, the cooling performance of three novel shaped solar panels, namely as pyramid, hexagonal and were simulated and compared. These novel shapes can be widely used in domestic areas (streets and solar farms) without the requirement of tracking systems. On the other hand, these towers have a lateral area which has been covered with a solar panel and equals as twice the infrastructure area, which is very suitable for urban areas. It is noteworthy that when the flat plate solar panels are organized in flat form they need an infrastructure more than panels area. They are also a proper choice when considering the urban design, as they appear same as modern residential buildings. The hypotheses applicable to the present study are for areas near the equator as well as for the middle of the day, which results in relatively homogeneous sunlight on all lateral surfaces of the towers. Through the present investigation the authors have evaluated the effect of **geometry** on the **temperature distribution** and **efficiency and power output** of the solar Panels. The previously published paper (Abu Hamdeh et al. [33]) has only considered the effect of amount of heat flux and inlet velocity of the coolant air. As is aware, the geometry is one of the major factors affecting on the thermal performance and efficiency of solar panels. Consequently, investigations on the influence of the variation of the geometry of the solar panels is of importance.

2. Physical model

2.1. Definition of the physical model

Fig. 1 presents the schematic of dimensions of the models considered in this study. As presented, the physical domain consists of

three solar panels shaped in pyramid, hexagonal, and conical forms. All the shapes exhibit the same lateral surface, which corresponds to 209.963 m^2. The shapes were considered to be under three constant heat flux values of 250 w/m^2, 500 w/m^2 and 750 w/m^2 (The three values were selected to simulate the effect of different solar radiation values during a day). The structures were cooled via air that entered from the trap door at the bottom side of the solar panel. The area of the trap door was 20 m^2 for all three cases considered in this study. After cooling the surfaces under heat flux, the coolant air exits from the trap door at the top of each shape. The thermo-physical properties of the coolant air were considered as constant. For each shape with a constant heat flux, three air mass flow rates of 0.24 kg/s, 2.4 kg/s, and 24 kg/s were considered to simulate the effect of mass flow rate on the cooling performance of each shape. Furthermore, the different cases analyzed in this work are briefly presented in Table 1. It should be noted that the regions near the quarter of the planet earth where the sun shines almost perpendicular to the earth are very potential to the proposed design. This mode could be effectively used to increase the radiation receiving surface in comparison with the area needed to stablish the solar cells with ordinary designs. This mode could be effectively used inside the cities or on top of the building roof to provide the needed electrical energy to an especial domestic usage.

2.2. Governing equations

In the present study, the flow was assumed to be steady and incompressible. Furthermore, the flow regime was considered as

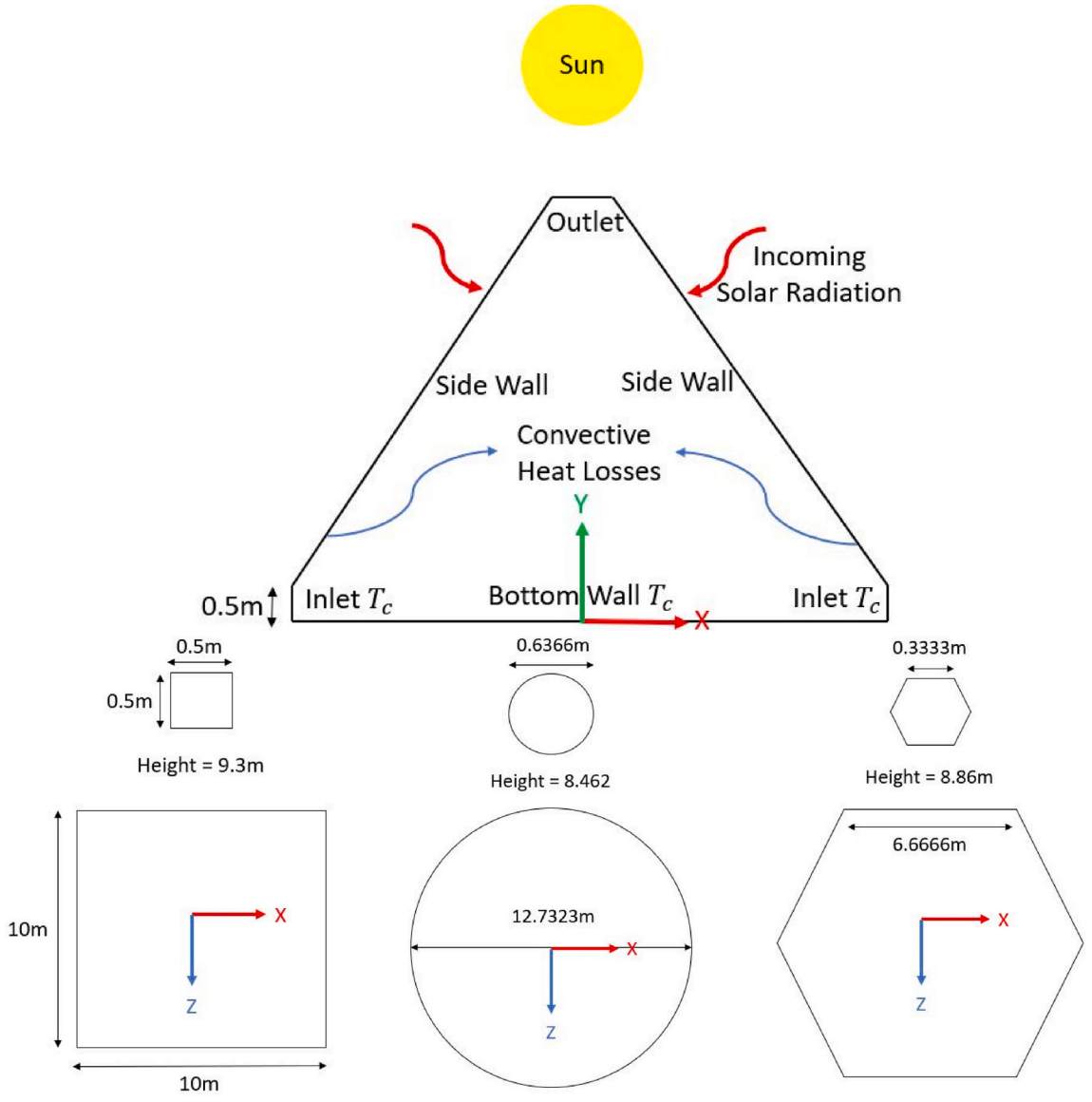

Fig. 1. Schematic of the geometrical properties of the three shapes (pyramid, hexagonal and conical) considered for PV solar panels.

Table 1
Characteristics of the different shapes considered in this study.

Structure	Heat flux (W/m^2)	Mass flow rate (kg/s)	lateral surface (m^2)	Area of inlet trap doors (m^2)
Pyramid	250, 500, 750	0.24, 2.4, 24	209.963	20
Hexagonal	250, 500, 750	0.24, 2.4, 24	209.963	20
Conical	250, 500, 750	0.24, 2.4, 24	209.963	20

turbulent. As mentioned earlier, the thermo-physical properties of the working fluid were assumed as constant. Also, the radiation effects were ignored while the boundary condition was determined to be the constant heat flux on the lateral surface of the solar panels. Thus, by considering the aforementioned assumptions, the governing equations associated with conservation of mass (1), conservation of momentum (2, 3, and 4, related to x, y and z directions, respectively) and conservation of energy (5) could be stated as follows [34–38]:

$$\frac{\partial u}{\partial x}+\frac{\partial v}{\partial y}+\frac{\partial w}{\partial z}=0 \tag{1}$$

$$u\frac{\partial u}{\partial x}+v\frac{\partial u}{\partial y}+w\frac{\partial u}{\partial z}=-\frac{1}{\rho}\frac{\partial p}{\partial x}+v\left(\frac{\partial^2 u}{\partial x^2}+\frac{\partial^2 u}{\partial y^2}+\frac{\partial^2 u}{\partial z^2}\right) \tag{2}$$

$$u\frac{\partial v}{\partial x}+v\frac{\partial v}{\partial y}+w\frac{\partial v}{\partial z}=-\frac{1}{\rho}\frac{\partial p}{\partial y}+v\left(\frac{\partial^2 v}{\partial x^2}+\frac{\partial^2 v}{\partial y^2}+\frac{\partial^2 v}{\partial z^2}\right)-g\beta(T-T_c) \tag{3}$$

$$u\frac{\partial w}{\partial x}+v\frac{\partial w}{\partial y}+w\frac{\partial w}{\partial z}=-\frac{1}{\rho}\frac{\partial p}{\partial z}+v\left(\frac{\partial^2 w}{\partial x^2}+\frac{\partial^2 w}{\partial y^2}+\frac{\partial^2 w}{\partial z^2}\right) \tag{4}$$

$$u\frac{\partial T}{\partial x}+v\frac{\partial T}{\partial y}+w\frac{\partial T}{\partial z}=\alpha\left(\frac{\partial^2 T}{\partial x^2}+\frac{\partial^2 T}{\partial y^2}+\frac{\partial^2 T}{\partial z^2}\right) \tag{5}$$

In the above equations, the term $u.v$ and w denote the velocity components related to x, y, and z directions, respectively. Furthermore, ϑ and ρ denote the kinematic viscosity and density of the flow, respectively. In the energy equation, parameters T and α denote the absolute temperature and thermal diffusivity of the working fluid, respectively.

In the present study, the dimensionless parameters are as follows [33,39,40].

$$\begin{gathered} X=\frac{x}{H},\ Y=\frac{y}{H},\ U=\frac{u}{\alpha/H},\ V=\frac{v}{\alpha/H},\ W=\frac{w}{\alpha/H},\ P=\frac{p}{\rho\left(\frac{\alpha}{H}\right)^2}, \\ \theta=\frac{T-T_c}{T_h-T_c},\ U=\frac{u}{\alpha/H},\ P_r=\frac{v}{\alpha},\ Ra=\frac{g\beta(T_h-T_c)H^3}{\nu\alpha} \end{gathered} \tag{6}$$

The mean convective heat transfer coefficient was calculated via the following equation [33,41].

$$\overline{h_c}=\frac{-k}{L(T_w-T_c)}\int_0^L\frac{\partial T}{\partial n}dl \tag{7}$$

2.3. Boundary condition

In the present study and for all the cases presented in Fig. 1, the mass flow inlet boundary condition with certain temperature was used for the coolant air and at the inlet trapdoor (bottom side). At the lateral surfaces and for the thermal boundary condition, constant heat flux was exerted. The boundary condition used for the velocity on the lateral surface of the solar panels was set to be "no slip". Furthermore, the outlet boundary conditions were assumed for the exit trap door (top of the solar panel). Additionally, the temperature of inlet air and bottom side of the solar panel were assumed as equal. Table 2, summarized the mentioned boundary conditions for each surface.

Table 2
Boundary conditions considered in this investigation.

Surface name	Thermal boundary conditions	Hydrodynamic boundary condition
Inlet trapdoors	Constant temperature	Mass flow inlet
Outlet trapdoors	–	Outlet flow
Lateral surfaces	Constant heat flux	No slip boundary conditions
Bottom side	Constant temperature	No slip boundary condition

3. Calculation process

The present study was performed via an open source CFD software (Open foam version 2.3.1). The Buoyant Boussinesq Pimple Foam solver was employed in present study. Although this solver considers the flow as unsteady, the nature of this study was steady. Hence, the results are related to the time when time independence was realized.

The turbulence model used in this study corresponded to the $k-\varepsilon$ (shear stress transport) model with a wall function [42]. Due to use of wall function, the y^{+} was considered as 64.4 for this model. Furthermore, the PISO algorithm was used for pressure and the

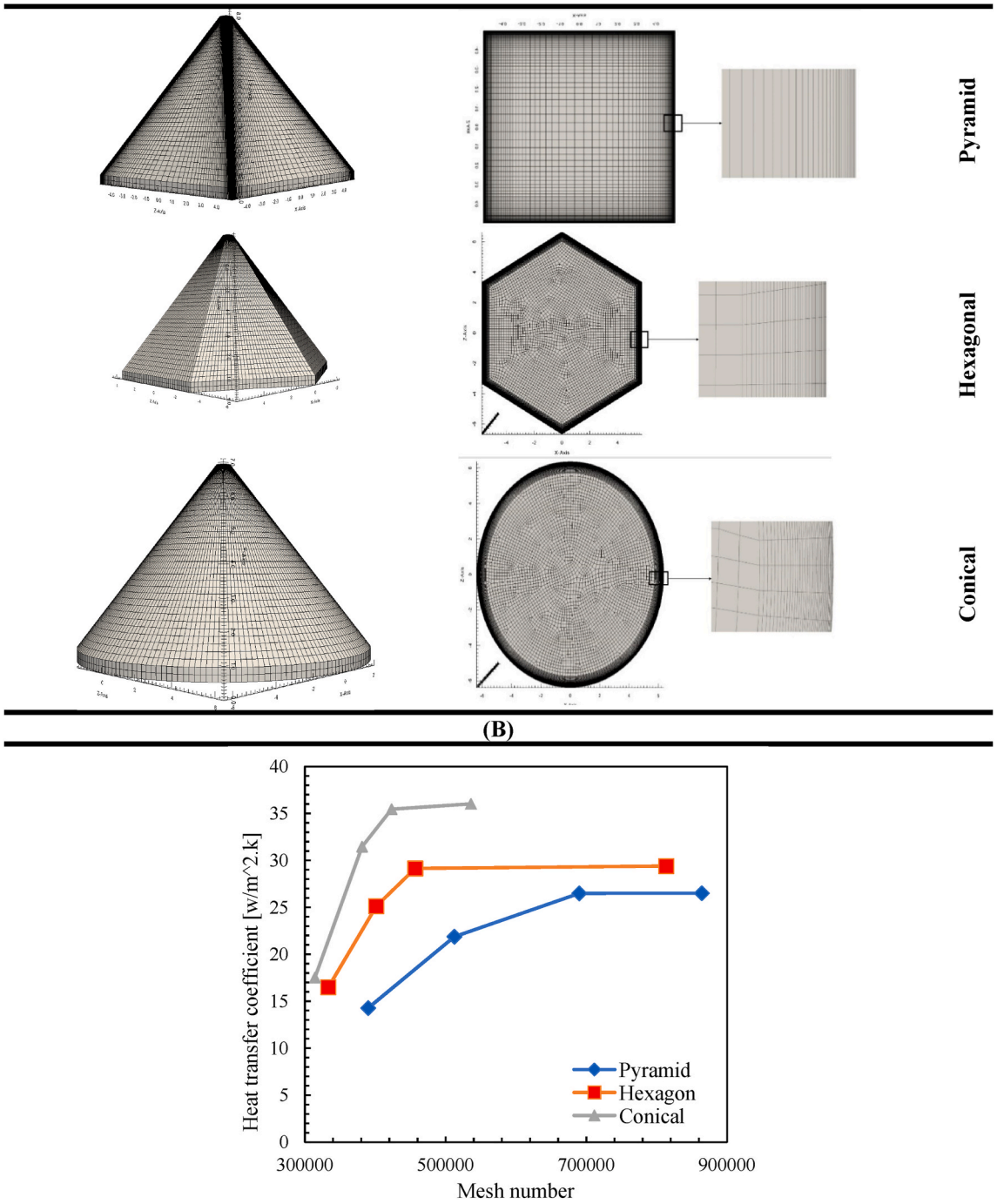

Fig. 2. A) Calculation domain for the pyramid, hexagonal, and conical shaped solar panels; B) Verification of mesh independence. (Variation in heat transfer coefficient vs number of cells for pyramid, hexagonal and conical shaped solar panels).

Navier–Stokes equations coupling [43]. The Gradient, Divergence, and Laplacian terms of the governing equations were discretized via an upwind second order scheme. Additionally, the Courant number was determined to be less than unit to enhance the convergence of the solution.

3.1. Grid description and grid independency check

Fig. 2A presents the calculation domain for the three geometrical structures. As shown in the figure, the non-homogenous cubic shaped cells were used for meshing the domain. Given that the size of the geometrical domain was significantly bigger than that of the boundary layer, a growth ratio was applied to mesh each geometry to mesh the near side area of the shapes. This implies that the cells near the lateral surface of shapes were smaller than those in near core regions. When going through the inner side of the shapes, the cells grow, and the size of the cells increases. The height of first cells, which were on lateral surface of the geometries, was constant for all shapes and corresponded to 50 μm.

Four different numbers of cells were used for each geometry to ensure mesh independence. The cases were examined at the most critical values of the variant parameters wherein the mass flow rate and heat flux were 24 kg/s and 750 w/m^2, respectively. To ensure the mesh independence of each geometry, the behavior of the heat transfer coefficient was analyzed. Fig. 2B shows the variation of heat transfer coefficient with respect to different number of cells for the three different geometries. The number of cells at which each geometry realized mesh independence condition varied for each geometry. For the pyramid shaped panel, the number of cells required to realize mesh independency corresponded to 864320, 813694, 536025 and 390000, respectively. Also, for the hexagonal shaped panel, four numbers of 333369, 401000, 457000 and 813000 were used. Furthermore, for the Conical panel, the cell numbers of 340000, 381000, 423000 and 536000 were used too. It should be noted that to save the calculation costs, the cell numbers used for conducting the rest of investigation were chosen to be 813694, 457000 and 423000 for the Pyramid, Hexagonal and Conical shaped panels, respectively.

3.2. Validation

This section addresses the validation of the present study. The validation was performed for the pyramid shaped structure. In this study, the size of the geometry was in real dimensions and the dry air was used as the working fluid (as coolant). Due to low Prandtl number of the working fluid, the magnitude of the thermal boundary layer formed on the lateral surface was small when being compared with the dimensions of the whole geometry. This ensureed that no interactions would occur between the boundary layers formed on two sides of the pyramid. Consequently, each of the pyramid sides is assumed as a free surface. Hence, at lower air mass flow rates (0.24 kg/s), the formation of large vortices and their domination due to free convection is highly probable which results in erroneous results. Consequently, the validation was conducted for air mass flow rate of 24 kg/s and for various heat fluxes. To obtain the heat transfer coefficient, equations (12)–(14) have been used.

$$Nu_x = 0.0308 Re_x^{4/5} Pr^{1/3} \tag{12}$$

$$\left(\overline{T}_s - T_\infty\right) = \frac{1}{L}\int_0^L (T_s - T_\infty)dx = \frac{q_s''}{L}\int_0^L \frac{x}{kNu_x}dx = \frac{q_s''}{k\overline{Nu}_L} \tag{13}$$

By calculating the $\overline{Nu}_L$ from equation (13), the surface averaged heat transfer coefficient can be derived from equation below:

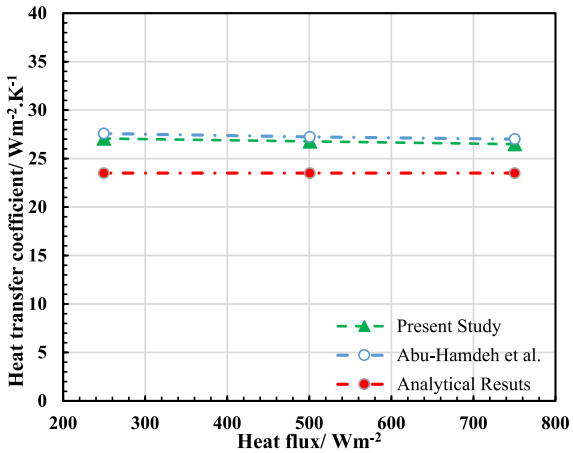

Fig. 3. Comparison between present study and the work of Abu-Hamdeh et al. [33] and analytical results [44].

$$Nu = \frac{hl}{k} \tag{14}$$

To ensure the validity of the numerical method, the results have also been compared with the results obtained by Abu-Hamdeh et al. [33]. Fig. 3 depicts the comparison of the results obtained in this study and those of Abu-Hamdeh et al. [33] and the analytical study. It should be noted that the paper published by Abu-Hamdeh et al. [33] has focused on the evaluation of the effect of inlet velocity of the coolant air and its' relation with the applied heat flux in a fixed geometry. However, the present investigation has focused on the influence of the geometry of the solar panel which was not conducted before. Since, the variation of geometry affects the creation of vortices, flow field and temperature distribution. The variation of these parameters directly affects performance of the solar panel.

The results obtained in this study and analytical results were in good agreement. The maximum error was approximately 15.35%. Also, the maximum deviation between the results of present investigation and the results of Abu-Hamdeh et al. [33] was less than 3%. The numerical study results were greater than those of analytical solution. This is because of presence of the small vortices generated at the lower section of the pyramid. Furthermore, it is important to note that the heat transfer coefficient on the free surface is independent of the heat flux, and this is clearly evident in the numerical results presented in Table 2. This indicates that the results obtained in the present study are credible.

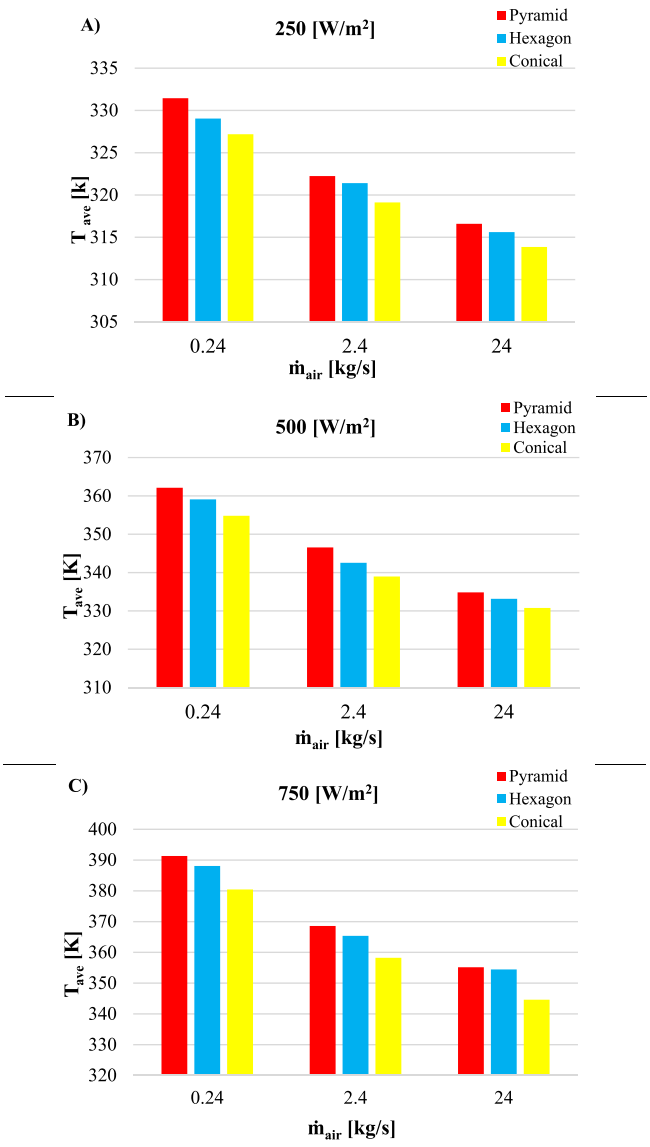

Fig. 4. Variation in average back-side temperature vs mass flow rate for different shapes (pyramid, hexagonal, and conical) at different heat fluxes (A, B, and C).

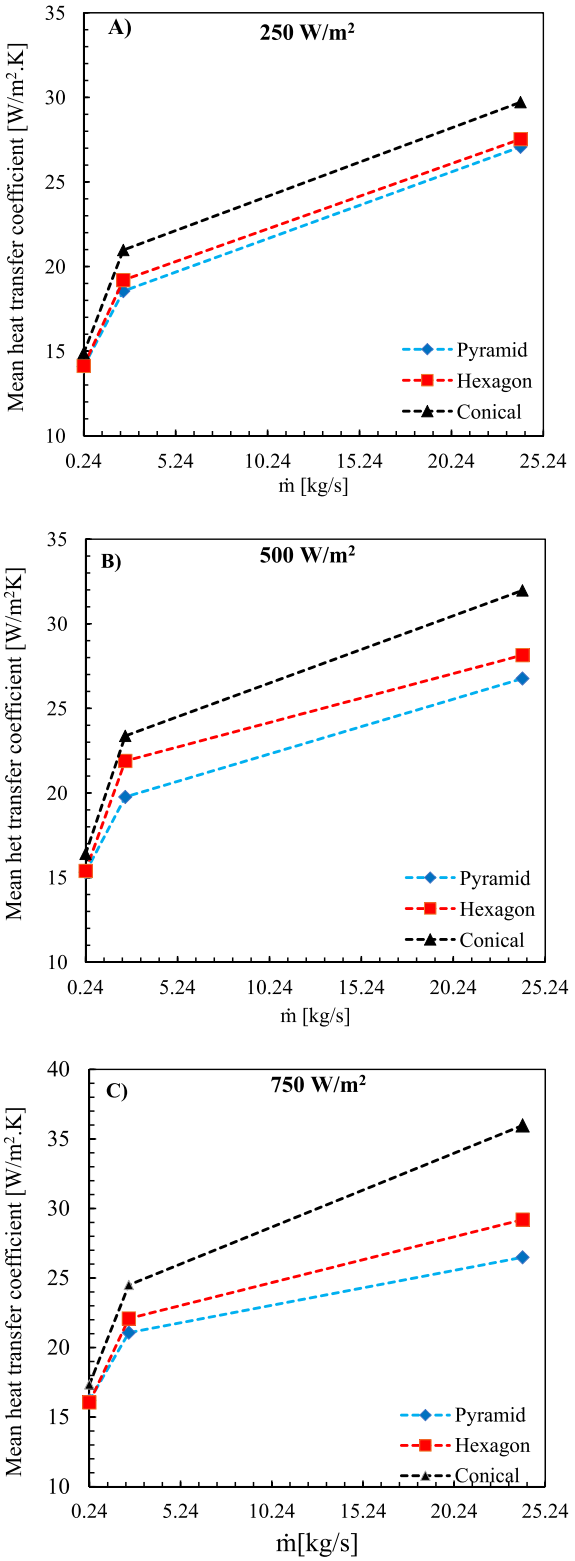

Fig. 5. Variation in average heat transfer coefficient vs mass flow rate for different shapes (pyramid, hexagonal, and conical) at different heat flux values (A, B and C).

4. Results and discussion

In the following section, the simulation results of the three geometries are discussed. In the present study, the thermal performances of the three novel-shaped solar panels are simulated, investigated, and compared. The shapes were in form of a pyramid, hexagon, and cone. All the shapes exhibit equal lateral surface that are under constant heat flux. The simulations were performed for steady conditions. To simulate different hours of a day, three different amounts of heat flux were applied on the lateral surface of each panel. The solar panels were cooled at each constant heat flux via air with three mass flow rates. The inlet air temperature was constant and was considered to be 20 °C.

The rest of the following section is divided into 2 subsections. The first subsection deals with the thermal properties of the considered shapes. In the second subsection, the effect of the shapes and cooling method on the efficiency and power output of the proposed solar panels is discussed.

4.1. Thermal performance

Fig. 4 demonstrates the variation in the average back-side temperature of the three shapes with respect to the mass flow rate of the cooling air. As the air mass flow rate increases, the back-side temperatures for all the shapes significantly decrease. For all the cases of heat flux values and air mass flow rates, the maximum and minimum back-side temperatures corresponded to the pyramid-shaped and conical-shaped solar panels, respectively. Additionally, for all the cases, the minimum back-side temperature corresponded to the conical-shaped solar panel. The maximum temperature difference between the proposed shapes was between the conical-shaped and pyramid-shaped solar panels, and the difference was approximately 10.9 °*C*. The maximum temperature difference was observed for the case with a heat flux and air mass flow rate of 750 W/m^2 and 0.24 kg, respectively. Additionally, it should be noted that even for the cases with heat flux values of 250 W/m^2 and 500 W/m^2, the maximum temperature difference was between the conical and pyramid shaped solar panels. This reveals that the changes in the shape of solar panels are more effective at low coolant air flow rates.

Given that the lateral surface of all the shapes and the mass flow rates of coolant air and heat flux values for all the cases are equal, the higher reduction in average back-side temperature of the conical shaped solar panel (when compared to other shapes) is due to the effect of the geometry of the conical panel on the heat transfer coefficient. Fig. 6 (A, B, and C) present the variation in heat transfer coefficient with respect to the various cases analyzed in this study.

As presented in Fig. 5, the heat transfer coefficients for all the shapes at all heat flux rates increase as the mass flow rate increases.

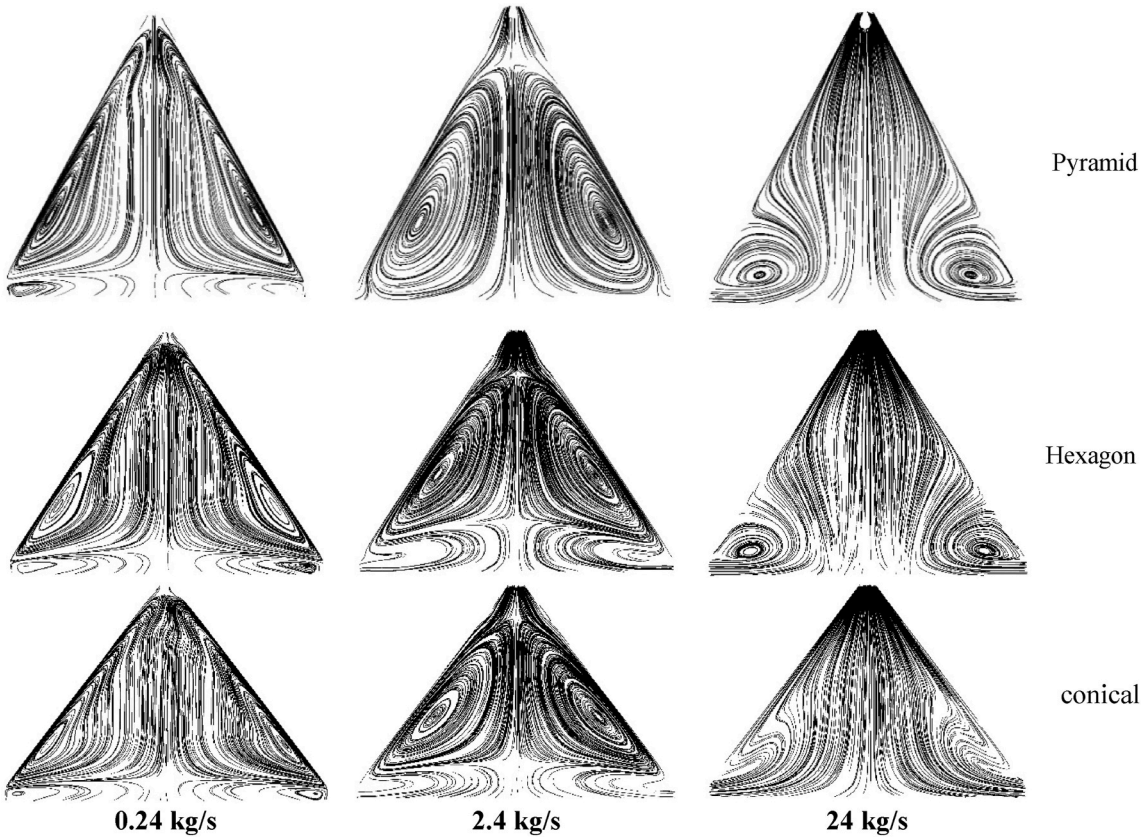

Fig. 6. Flow streamlines for the different geometrical shapes at different mass flow rates.

Furthermore, the results in Fig. 5 (A, B and C) show that the heat transfer coefficient of hexagonal shaped solar panel is greater than that of the pyramid shaped solar panel. Additionally, the heat transfer coefficient of the conical shaped solar panel is higher than that of the hexagonal shaped solar panel. The maximum improvement ratio of the heat transfer coefficient was between the conical shaped and pyramid shaped solar panels, and it was approximately 19%. This ratio was observed at heat flux and mass flow rate of 750 W/m^2 and 24 kg/s, respectively.

The higher improvement in the heat transfer coefficient of conical shaped solar panel when compared to those of other shapes can be explained as follows: The heat transfer coefficient is dependent on flow characteristics and geometrical properties of the surface. The higher improvement in the heat transfer coefficient of conical shaped solar panel when compared to those of other cases can be explained by the temperature distribution and flow stream lines, which are presented in Figs. 6 and 7.

Fig. 6 presents the streamlines related to the different geometries of the solar panels. It is to be mentioned that the streamlines presented in Fig. 6 are those that occur on the vertical bisector of the shapes due to the asymmetric feature of the geometries. Fig. 6 reveals that bigger vortices are generated in pyramid shaped solar panel when compared to those in hexagonal and conical shaped solar panels. These vortices are not very powerful. So they may exhibit a laminar regime. As the air mass flow rate increases at the pyramid shaped solar panel, a big vortex is generated. The vortex covers the entire length of the side of the pyramid. At a mass flow rate of 2.4 kg/s for the hexagonal and conical shaped solar panels, the size of the vortex diminishes when compared to that of pyramid shaped panel. Furthermore, the intensity of the streamlines increased, especially near the side regions of the solar panels. Indeed, through the Pyramid shaped solar panel and at each side of panel, there is only one face that the coolant air slides on it, however, for the Hexagonal panel this number increases. In fact, the normal vector of these faces are not parallel to each other, consequently, the returned air flow from these faces coincide with each other which causes interruption inside the layers of the fluid flow. These interruptions play the major role on the formation of the vortices and increases the turbulence intensity of the flow associated to each shape. For the conical shaped panel, due to the circular nature of the surfaces, the coincidence of the returnee flows from the side walls are intensified. Consequently, the streamlines get denser form in this shape and causes to more increment in the turbulence intensity of the flow. At an air mass flow rate of 24 kg/s, it could be seen that the size of the vortices of the Hexagonal panel is smaller than that in Pyramid panel. Also, for the conical shaped panel, no vortex was generated. It should be mentioned that for the Pyramid and

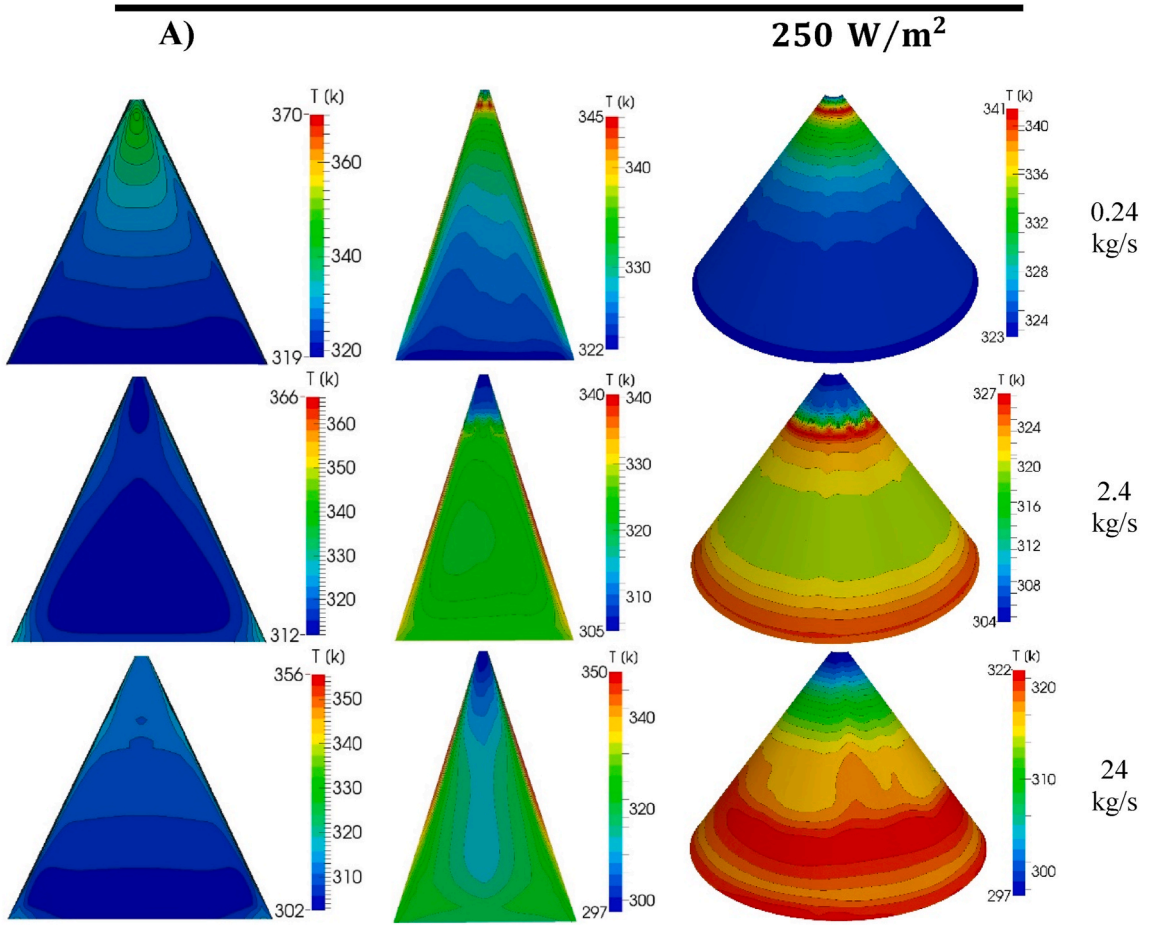

Fig. 7. Contours of temperature for various cases analyzed in the study.

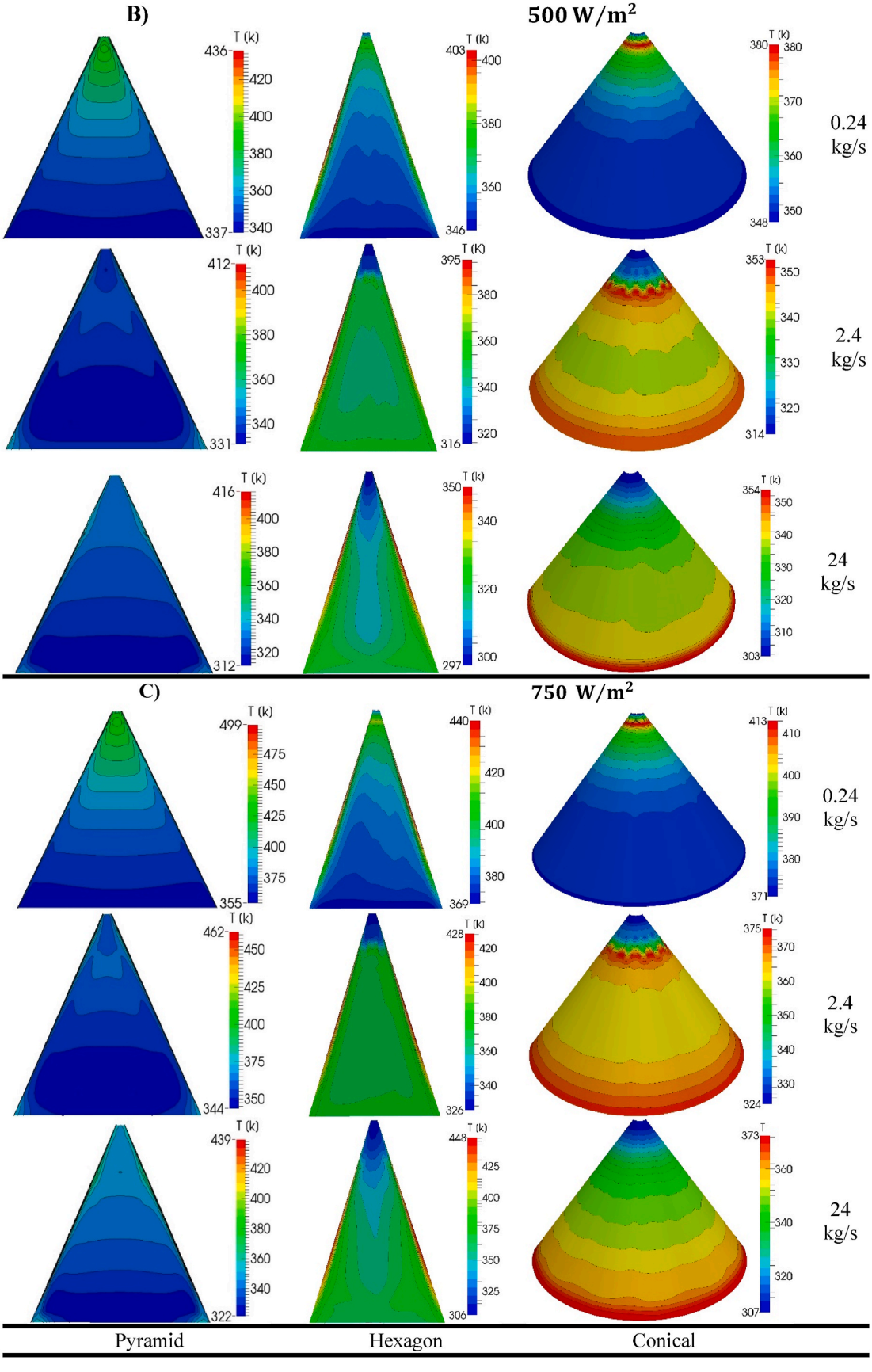

Fig. 7. (*continued*).

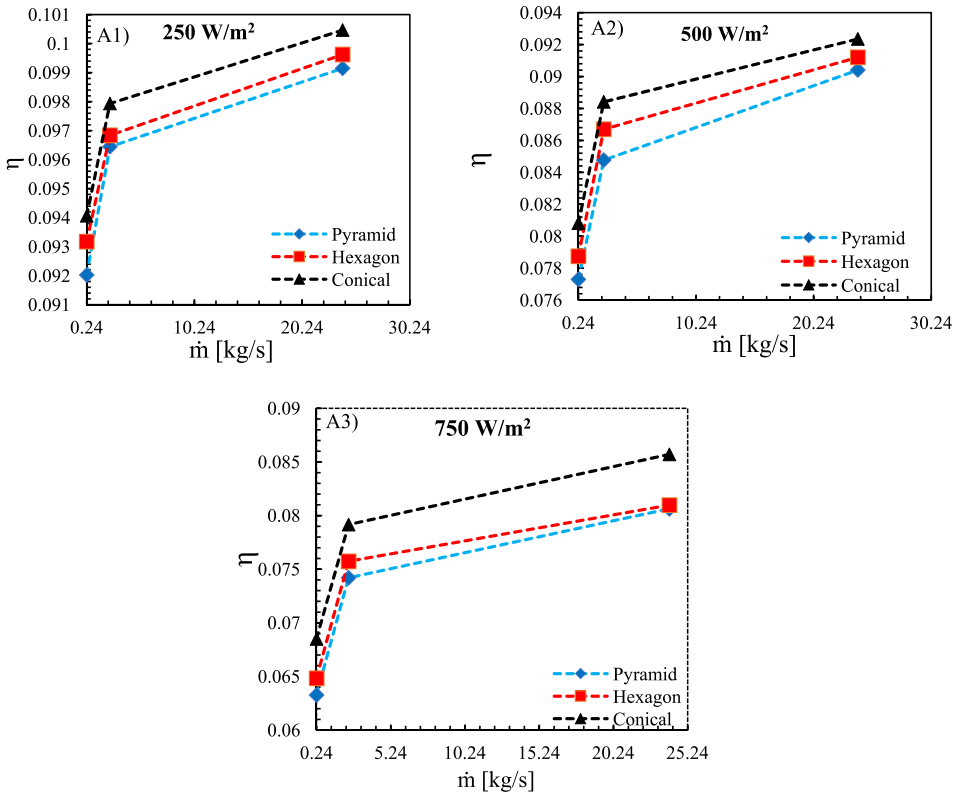

(caption on next page)

Fig. 8. A1, A2 and A3: Variation in efficiency of solar panel vs air mass flow rate for different shapes at varying heat flux values; B1, B2 and B3: variation of power output of each solar panel vs air mass flow rate for different shapes at varying heat flux values.

Hexagonal shaped panels, the lower parts of the side walls have more width than the top part, which allows for the creation of the vortices. For the Hexagonal shaped this width is less than that of Pyramid form consequently, the streamlines get denser and the size of vortices diminishes. However, there is no flat area for the conical shaped panel. Consequently, the interruption of the air streams is more often and the size of vortices diminishes and circulating flow gets destroyed. This implies that the entire inlet stream of the flow exits from the top trapdoor before any circulation occurs. In many previous studies, the vortex is proposed as an element of heat transfer enhancement. However, it should be noted that vorticities that exhibit a 2-D nature and circulate in a laminar form can act as a bulk of fluid, which is trapped in a region. This type of movement leads to a loss of heat transfer capacity of the working fluid (by reaching the temperature of the heating part). Subsequently, the cooling capability of the fluid is decreased. Based on the above explanations and by comparing the flow behaviors in Figs. 5 and 6, it can be concluded that the change in the structure of the solar panel from pyramid shape to conical shape affects the form of flow, which in turn positively affects the heat transfer rate of the solar panel.

Fig. 7 depicts the temperature contours (isotherm lines) for the three structures. As mentioned before, the back-side temperature of the solar cell plays a crucial role in electricity production efficiency of the solar panel. Hence, understanding the temperature distribution of the solar panel can aid in controlling the cooling process in an optimal manner. The maximum temperature of the hexagonal shaped solar panel is less than that of the pyramid shaped panel for almost all the cases. Simultaneously, the maximum temperature of the conical shaped solar panel is less than those of the other two structures for all the cases with varying heat fluxes and mass flow rates. The contours of temperature reveal that stratified distribution of temperature occurs for all cases with an air mass flow rate of 0.24 kg/s. It should be noted that this finding was in agreement with the results of Abu-Hamdeh et al. [33] at which they also indicated that inside the Pyramid shaped solar panel the stratified distribution of the temperature is very dominant. In these cases, the maximum temperature occurs at a region near the exit trapdoor. Fig. 6 shows that this point (where the maximum temperature occurs) is the same point where the flow in the vortices turns towards the downward side. At a mass flow rate of 2.4 kg/s, the stratified form of temperature distribution still remains for the solar panel with pyramid shape. At this flow rate, the maximum temperature occurs at the corners of the pyramid shaped and hexagonal shaped solar panels. At these regions, the circulating air flow is trapped due to the existence of vortices. Consequently, air loses its heat transfer capacity. However, for the conical shaped solar panel, the temperature is distributed more evenly when compared to that in the other two shapes. In the conical shape, the maximum temperature occurs at two regions. The first region is near the bottom side and the second region is near the exit trapdoor of the solar panel. As mentioned earlier, at these regions, the flow direction of the vortices changes and the intensity of the flow streamlines is maximum. In these regions, the flow heat transfer coefficient decreases. Thus, the solar panel back-side temperature increases. For the cases with mass flow rate of 24 kg/s, the distribution of temperature remains in the stratified form for the pyramid shaped and hexagonal shaped solar panels. The maximum temperature of the pyramid shaped panel was less than those for cases with a mass flow rate of 2.4 kg/s and all heat flux values. However, for the hexagonal shaped solar panel, the maximum temperatures of cases with air mass flow rate of 24 kg/s were greater than those of cases with air flow rate of 2.4 kg/s. This increment in the maximum temperature in certain cases (cases with a heat flux of 750 W/m^2) was uniform up to 20 °C. For the conical shaped solar panel at an air mass flow rate of 24 kg/s, the maximum temperature of the solar panel was less than that at air mass flow rate of 2.4 kg/s. In this case, the stratified distribution of flow was maintained. Fig. 6 shows that a circulating flow occurs at lower region of the conical shaped solar panel and near the lateral surface of the solar panel. By comparing the isotherm figures of conical shaped solar panel at a mass flow rate of 24 kg/s with those related to streamline (Fig. 6), it is evident that the concentration of high temperature curves occurs in the lower region. Another noteworthy point is about the density of the distribution of temperature: As mentioned through the introduction section, the uniform distribution of the temperature is very important for the enhancement of the performance of the solar panel [32]. Looking to the temperature contours of Fig. 7, it is revealed that the conical shaped panel not only has less values of the temperature but also the distribution of the temperature is more even than other shapes. Indeed, local increments of the temperature diminish the efficiency of the panel and cause to early breakdowns of the PV panels. This point denotes that the conical shaped panel not only could enhance the efficiency of the panel but also could reduce the repairement costs and increase the life of PV panel.

4.2. Efficiency and power output analysis

The cooling of the solar panels significantly affects the efficiency of the PVs. Many researchers attempted to formulate the effect of heat transfer on the efficiency of the PVs. Some researchers reported that an increment of 1 °C in the back-side temperature of the solar panel cell leads to a reduction in efficiency of the solar panel by 0.5%. The following equation has been proposed [3,4] to predict the effect of back-side temperature on the efficiency of the solar panel.

$$\eta_{pv} = \eta_{TR}\left(1 - \beta_R(T_C - T_R)\right) \tag{15}$$

In this equation, η_{TR} denotes the PV module efficiency measured at the reference temperature, β_R denotes the coefficient of temperature for the efficiency of the cell. Furthermore, T_C and T_R denote the cell temperature and reference temperature, respectively.

Fig. 8, A1, A2 and A3 shows the variation in the efficiency of the three shapes of the solar panels with respect to different cases considered in this study. By increasing the air mass flow rate, the efficiency of all the shapes of solar panels increases. For the cases with

a heat flux of 250 W/m^2 (Fig. 8 A), the maximum efficiency was 0.100, which was exhibited by the conical shaped solar panel at an air mass flow rate of 24 kg/s. The efficiency of the solar panel with conical shape for this case was higher by 2.8% when compared to the efficiency of the pyramid shaped solar panel with same condition. For the cases with a heat flux of 500 W/m^2, as the air mass flow rate increases, the efficiency of the solar panel increases. Similarly, for the cases with the heat flux of 250 W/m^2, the efficiency of the hexagonal shaped solar panel was greater than that of the pyramid shaped panel. Furthermore, the efficiency of the conical shaped panel was higher than those of the other two shapes. The maximum efficiency of the conical solar panel was observed at a mass flow rate of 24 kg/s and was approximately 0.0923. This was higher by 5.54% when compared to that of the pyramid shaped panel. For the cases with a heat flux of 750 W/m^2, the behavior of the efficiency curves was similar to that of the two aforementioned cases. However, in this case, the maximum efficiency was approximately 0.085. Similar to the aforementioned cases, this value was observed at a mass flow rate of 24 kg/s and was exhibited by the conical shaped solar panel. It is worth mentioning that the increment ratio of the efficiency related to this case was approximately 8.26%. A comparison of this increment ratio with the values of the decrement in the back-side temperature of the solar panel, reveals that the relationship between the increment ratio and back-side temperature is in agreement with the statement in previous studies [9]. As per previous studies, an increment of 1 °C in the back-side temperature leads to a reduction in efficiency by approximately 0.5%, and vice versa.

Fig. 8 B1, B2, B3 presents the variation of output power for the different cases investigated in the present study. The power output values were calculated via the following equation [11]:

$$Q_{ave} = A \sum \eta_i I_i \Big/ N_d \tag{16}$$

where the term A is the receiving surface of the PV, the η_i is the efficiency of the PV panel which was calculated by equation (15). Besides, the term I_i/N_d is the average of the radiation within a year.

As presented in Fig. 8 B1, B2, and B3, the output power of each of the cases considered in this study increases by the increment of the air inlet mass flow rate. It is evident that the power output of the conical shaped panel is more than other cases almost in all condition. It should be noted that the difference between the output power of conical shaped panel and other cases increases by the increment of the air mass flow inlet. The maximum power output was related to the conical shaped panel and was about 13500 W which has been achieved for the radiation values of 750 W/m^2 where the air mass flow rate was 24 kg/s It should be noted that the temperature distribution of the conical shaped panel is the main reason of the increment of the output power of conical panel in comparison with other cases. Indeed, the less values of back side temperature of the panel and even distribution of the temperature along the panel enhances the efficiency of the PVs which directly increases the power output of the panel. As mentioned before, the conical shaped panel causes to reduction of the laminar form of the vortices that causes to trapping of the cooling air in a certain area. Consequently, by continues passing of the cooling air over the certain area the temperature of the back side of panel reduces and results in enhancement in the output power of the panel.

5. Conclusions

In this work, the cooling performance of the three novel shaped solar panels, namely pyramid, hexagonal, and conical, was simulated and compared. The simulation process was performed via an open source CFD software (Open foam, Version 2.3.1). The simulation was performed for the steady condition, and the fluid flow was considered to be incompressible. The $K-\varepsilon$ model was used for modeling the turbulence feature of the flow. Instead of solar radiation, a constant heat flux was applied on the lateral surface of the solar panel. Furthermore, air at a constant temperature of 293 K was injected from the bottom trap door to cool the lateral surface of the solar panels. The main findings of the study are as follows:

- The conical shaped solar panel exhibited minimum mean temperatures for all the cases considered in this study.
- High temperatures for the pyramid shaped and hexagonal shaped solar panels were distributed near the corners. These regions should be cooled via other techniques when considering these designs for real applications.
- The distribution of high temperature for the conical shaped solar panel in cases with an air mass flow rate of 2.4 kg/s and 24 kg/s occurred in a more expanded area than those for the two other shapes. This area can be easily cooled via various techniques that can be applied to surfaces.
- The heat transfer coefficient of conical shaped solar panel was as high as 23% and 35% more than those of hexagonal shaped and pyramid shaped solar panels, respectively.
- The conical shaped solar panel exhibited 8.4% and 5% higher efficiency than the pyramid shaped and hexagonal shaped solar panels, respectively.
- The distribution of the temperature in the conical shaped panel was more even than other shapes. This point denoted that the conical form could provide both better performance and more working life time for the PV panel.
- The maximum power output was about 13500 W and was related to conical shaped panel.

Research outlook of the present investigation

It is proposed that the upcoming investigations in this subject would investigate the effect of addition of internal grooves on the conical shapes. Furthermore, it is recommended to seek the effect of having different phase change material (fabricated on the back side of the panel) on the temperature distribution of the panels.

CRediT authorship contribution statement

Hamdi Ayed: Resources, Formal analysis, Investigation. **Hazim Moria:** Writing – review & editing, Writing – original draft, Investigation. **Fayez Aldawi:** Resources, Formal analysis. **Naeim Farouk:** Writing – review & editing, Conceptualization. **Kamal Sharma:** Writing – review & editing, Methodology, Formal analysis. **Mohammad Mehdizadeh Youshanlouei:** Software, Post processing. **Ibrahim Mahariq:** Writing – original draft. **Fahd Jarad:** Mesh generation.

Declaration of competing interest

The authors declare that they have no known competing financial interests or personal relationships that could have appeared to influence the work reported in this paper.

Acknowledgment

The authors acknowledge the Deanship of Scientific Research for providing administrative and financial support. Funding for this work has been provided by the Deanship of Scientific Research, King Khalid University, Ministry of Education, Kingdom of Saudi Arabia, under research grant award number RGP. 2/100/42."

References

[1] C. Jiang, L. Xiang, S. Miao, L. Shi, D. Xie, J. Yan, Z. Zheng, X. Zhang, Y. Tang, Flexible interface design for stress regulation of a silicon anode toward highly stable dual-ion batteries, Adv. Mater. 32 (2020) 1908470, https://doi.org/10.1002/adma.201908470.
[2] A. Yu, Q. Pan, M. Zhang, D. Xie, Y. Tang, Fast rate and long life potassium-ion based dual-ion battery through 3D porous organic negative electrode, Adv. Funct. Mater. 30 (2020) 2001440, https://doi.org/10.1002/adfm.202001440.
[3] K. Tan, Y. Qin, T. Du, L. Li, L. Zhang, J. Wang, Biochar from waste biomass as hygroscopic filler for pervious concrete to improve evaporative cooling performance, Construct. Build. Mater. 287 (2021) 123078, https://doi.org/10.1016/j.conbuildmat.2021.123078.
[4] X. Yan, X. Huang, Y. Chen, Y. Liu, L. Xia, T. Zhang, H. Lin, D. Jia, B. Zhong, G. Wen, Y. Zhou, A theoretical strategy of pure carbon materials for lightweight and excellent absorption performance, Carbon N. Y. 174 (2021) 662–672, https://doi.org/10.1016/j.carbon.2020.11.044.
[5] Y. Yang, H. Chen, X. Zou, X.-L. Shi, W.-D. Liu, L. Feng, G. Suo, X. Hou, X. Ye, L. Zhang, C. Sun, H. Li, C. Wang, Z.-G. Chen, Flexible carbon-fiber/semimetal Bi nanosheet arrays as separable and recyclable plasmonic photocatalysts and photoelectrocatalysts, ACS Appl. Mater. Interfaces 12 (2020) 24845–24854, https://doi.org/10.1021/acsami.0c05695.
[6] A. Khanlari, A. Sözen, F. Afshari, A.D. Tuncer, Energy-exergy and sustainability analysis of a PV-driven quadruple-flow solar drying system, Renew. Energy 175 (2021) 1151–1166, https://doi.org/10.1016/j.renene.2021.05.062.
[7] L. Tan, Y. Sun, C. Wei, Y. Tao, Y. Tian, Y. An, Y. Zhang, S. Xiong, J. Feng, Design of robust, lithiophilic, and flexible inorganic-polymer protective layer by separator engineering enables dendrite-free lithium metal batteries with LiNi0.8Mn0.1Co0.1O2 cathode, Small 17 (2021) 2007717, https://doi.org/10.1002/smll.202007717.
[8] A. Merida García, J. Gallagher, M. Crespo Chacón, A. Mc Nabola, The environmental and economic benefits of a hybrid hydropower energy recovery and solar energy system (PAT-PV), under varying energy demands in the agricultural sector, J. Clean. Prod. 303 (2021) 127078, https://doi.org/10.1016/j.jclepro.2021.127078.
[9] H.M.S. Bahaidarah, A.A.B. Baloch, P. Gandhidasan, Uniform cooling of photovoltaic panels: a review, Renew. Sustain. Energy Rev. 57 (2016) 1520–1544, https://doi.org/10.1016/j.rser.2015.12.064.
[10] J. Siecker, K. Kusakana, B.P. Numbi, A review of solar photovoltaic systems cooling technologies, Renew. Sustain. Energy Rev. 79 (2017) 192–203, https://doi.org/10.1016/j.rser.2017.05.053.
[11] M.D. Siegel, S.A. Klein, W.A. Beckman, A simplified method for estimating the monthly-average performance of photovoltaic systems, Sol. Energy 26 (1981) 413–418, https://doi.org/10.1016/0038-092X(81)90220-6.
[12] Y. Ruoping, Y. Xiaohui, L. Fuwei, W. Huajun, Study of operation performance for a solar photovoltaic system assisted cooling by ground heat exchangers in arid climate, China, Renew. Energy 155 (2020) 102–110, https://doi.org/10.1016/j.renene.2020.03.109.
[13] D.S. Cocco, A.M.S. Costa, Effect of a global warming model on the energetic performance of a typical solar photovoltaic system, Case Stud. Therm. Eng. 14 (2019) 100450, https://doi.org/10.1016/j.csite.2019.100450.
[14] D. Sato, N. Yamada, Review of photovoltaic module cooling methods and performance evaluation of the radiative cooling method, Renew. Sustain. Energy Rev. 104 (2019) 151–166, https://doi.org/10.1016/j.rser.2018.12.051.
[15] B. Zhao, M. Hu, X. Ao, G. Pei, Performance analysis of enhanced radiative cooling of solar cells based on a commercial silicon photovoltaic module, Sol. Energy 176 (2018) 248–255, https://doi.org/10.1016/j.solener.2018.10.043.
[16] E. Lee, T. Luo, Black body-like radiative cooling for flexible thin-film solar cells, Sol. Energy Mater. Sol. Cells 194 (2019) 222–228, https://doi.org/10.1016/j.solmat.2019.02.015.
[17] A. Saxena, S. Deshmukh, S. Nirali, S. Wani, Laboratory based experimental investigation of photovoltaic (PV) thermo-control with water and its proposed real-time implementation, Renew. Energy 115 (2018) 128–138, https://doi.org/10.1016/j.renene.2017.08.029.
[18] M. Javidan, A.J. Moghadam, Experimental investigation on thermal management of a photovoltaic module using water-jet impingement cooling, Energy Convers. Manag. 228 (2021) 113686, https://doi.org/10.1016/j.enconman.2020.113686.
[19] F. Bayrak, H.F. Oztop, F. Selimefendigil, Effects of different fin parameters on temperature and efficiency for cooling of photovoltaic panels under natural convection, Sol. Energy 188 (2019) 484–494, https://doi.org/10.1016/j.solener.2019.06.036.
[20] J.C. Mojumder, W.T. Chong, H.C. Ong, K.Y. Leong, Abdullah-Al-Mamoon, An experimental investigation on performance analysis of air type photovoltaic thermal collector system integrated with cooling fins design, Energy Build. 130 (2016) 272–285, https://doi.org/10.1016/j.enbuild.2016.08.040.
[21] F. Yazdanifard, M. Ameri, E. Ebrahimnia-Bajestan, Performance of nanofluid-based photovoltaic/thermal systems: a review, Renew. Sustain. Energy Rev. 76 (2017) 323–352, https://doi.org/10.1016/j.rser.2017.03.025.
[22] M.R. Salem, M.M. Elsayed, A.A. Abd-Elaziz, K.M. Elshazly, Performance enhancement of the photovoltaic cells using Al2O3/PCM mixture and/or water cooling-techniques, Renew. Energy 138 (2019) 876–890, https://doi.org/10.1016/j.renene.2019.02.032.
[23] S.R. Abdallah, I.M.M. Elsemary, A.A. Altohamy, M.A. Abdelrahman, A.A.A. Attia, O.E. Abdellatif, Experimental investigation on the effect of using nano fluid (Al2O3-Water) on the performance of PV/T system, Therm. Sci. Eng. Prog. 7 (2018) 1–7, https://doi.org/10.1016/j.tsep.2018.04.016.
[24] S.R. Abdallah, H. Saidani-Scott, O.E. Abdellatif, Performance analysis for hybrid PV/T system using low concentration MWCNT (water-based) nanofluid, Sol. Energy 181 (2019) 108–115, https://doi.org/10.1016/j.solener.2019.01.088.
[25] S. Alous, M. Kayfeci, A. Uysal, Experimental investigations of using MWCNTs and graphene nanoplatelets water-based nanofluids as coolants in PVT systems, Appl. Therm. Eng. 162 (2019) 114265, https://doi.org/10.1016/j.applthermaleng.2019.114265.

[26] U. Sajjad, M. Amer, H.M. Ali, A. Dahiya, N. Abbas, Cost effective cooling of photovoltaic modules to improve efficiency, Case Stud. Therm. Eng. 14 (2019) 100420, https://doi.org/10.1016/j.csite.2019.100420.
[27] A.E. Kabeel, M. Abdelgaied, R. Sathyamurthy, A comprehensive investigation of the optimization cooling technique for improving the performance of PV module with reflectors under Egyptian conditions, Sol. Energy 186 (2019) 257–263, https://doi.org/10.1016/j.solener.2019.05.019.
[28] N.A.S. Elminshawy, M. El Ghandour, H.M. Gad, D.G. El-Damhogi, K. El-Nahhas, M.F. Addas, The performance of a buried heat exchanger system for PV panel cooling under elevated air temperatures, Geothermics 82 (2019) 7–15, https://doi.org/10.1016/j.geothermics.2019.05.012.
[29] S.-Y. Wu, T. Wang, L. Xiao, Z.-G. Shen, Effect of cooling channel position on heat transfer characteristics and thermoelectric performance of air-cooled PV/T system, Sol. Energy 180 (2019) 489–500, https://doi.org/10.1016/j.solener.2019.01.043.
[30] L. Xu, J. Ji, J. Cai, W. Ke, X. Tian, B. Yu, J. Wang, A hybrid PV thermal (water or air) wall system integrated with double air channel and phase change material: a continuous full-day seasonal experimental research, Renew. Energy 173 (2021) 596–613, https://doi.org/10.1016/j.renene.2021.04.008.
[31] S. Golzari, A. Kasaeian, M. Amidpour, S. Nasirivatan, S. Mousavi, Experimental investigation of the effects of corona wind on the performance of an air-cooled PV/T, Renew. Energy 127 (2018) 284–297, https://doi.org/10.1016/j.renene.2018.04.029.
[32] Y. Amanlou, T. Tavakoli Hashjin, B. Ghobadian, G. Najafi, Air cooling low concentrated photovoltaic/thermal (LCPV/T) solar collector to approach uniform temperature distribution on the PV plate, Appl. Therm. Eng. 141 (2018) 413–421, https://doi.org/10.1016/j.applthermaleng.2018.05.070.
[33] N.H. Abu-Hamdeh, S. Khorasani, H.F. Oztop, K.A. Alnefaie, Numerical analysis on heat transfer of a pyramid-shaped photovoltaic panel, J. Therm. Anal. Calorim. (2021), https://doi.org/10.1007/s10973-021-10604-w.
[34] M. Zhang, X. Song, X. Ou, Y. Tang, Rechargeable batteries based on anion intercalation graphite cathodes, Energy Storage Mater. 16 (2019) 65–84, https://doi.org/10.1016/j.ensm.2018.04.023.
[35] X. Du, J. Qiu, S. Deng, Z. Du, X. Cheng, H. Wang, Flame-retardant and solid-solid phase change composites based on dopamine-decorated BP nanosheets/ Polyurethane for efficient solar-to-thermal energy storage, Renew. Energy 164 (2021) 1–10, https://doi.org/10.1016/j.renene.2020.09.067.
[36] M. Wang, Y. Tang, A review on the features and progress of dual-ion batteries, Adv. Energy Mater. 8 (2018) 1703320, https://doi.org/10.1002/aenm.201703320.
[37] Y. Zhang, G. Liu, C. Zhang, Q. Chi, T. Zhang, Y. Feng, K. Zhu, Y. Zhang, Q. Chen, D. Cao, Low-cost MgFexMn2-xO4 cathode materials for high-performance aqueous rechargeable magnesium-ion batteries, Chem. Eng. J. 392 (2020) 123652, https://doi.org/10.1016/j.cej.2019.123652.
[38] Y. Liu, Z. Wei, B. Zhong, H. Wang, L. Xia, T. Zhang, X. Duan, D. Jia, Y. Zhou, X. Huang, O-, N-Coordinated single Mn atoms accelerating polysulfides transformation in lithium-sulfur batteries, Energy Storage Mater. 35 (2021) 12–18, https://doi.org/10.1016/j.ensm.2020.11.011.
[39] J. Liu, Y. Yi, X. Wang, Exploring factors influencing construction waste reduction: a structural equation modeling approach, J. Clean. Prod. 276 (2020) 123185, https://doi.org/10.1016/j.jclepro.2020.123185.
[40] P. Wang, Z. Li, Q. Xie, W. Duan, X. Zhang, H. Han, A passive anti-icing strategy based on a superhydrophobic mesh with extremely low ice adhesion strength, J. Bionic Eng. 18 (2021) 55–64, https://doi.org/10.1007/s42235-021-0012-4.
[41] M.-W. Tian, S. Khorasani, H. Moria, S. Pourhedayat, H.S. Dizaji, Profit and efficiency boost of triangular vortex-generators by novel techniques, Int. J. Heat Mass Tran. 156 (2020) 119842, https://doi.org/10.1016/j.ijheatmasstransfer.2020.119842.
[42] R. Florian Menter, Two-equation eddy-viscosity turbulence models for engineering applications, Am. Inst. Aeronaut. Astronaut. 32 (1994) 1598–1605.
[43] R.I. Issa, Solution of the implicitly discretised fluid flow equations by operator-splitting, J. Comput. Phys. 62 (1986) 40–65, https://doi.org/10.1016/0021-9991(86)90099-9.
[44] F.P. Incropera, D.P. DeWitt, Fundamentals of heat and mass transfer. https://doi.org/10.1016/j.applthermaleng.2011.03.022, 1996, 890.